BIOLOGY OF REPRODUCTION (2013) **89**(1):6, 1–11
Published online before print 22 May 2013.
DOI 10.1095/biolreprod.113.108712

Plasma Membrane Ca^{2+}-ATPase 4 in Murine Epididymis: Secretion of Splice Variants in the Luminal Fluid and a Role in Sperm Maturation[1]

Ramkrishna Patel,[3,4] Amal A. Al-Dossary,[3,4] Deborah L. Stabley,[5] Carol Barone,[5] Deni S. Galileo,[4] Emanuel E. Strehler,[6] and Patricia A. Martin-DeLeon[2,4]

[4]*Department of Biological Sciences, University of Delaware, Newark, Delaware*
[5]*A.I. DuPont Hospital for Children, Wilmington, Delaware*
[6]*Department of Biochemistry and Molecular Biology, Mayo Clinic College of Medicine, Rochester, Minnesota*

ABSTRACT

Plasma membrane Ca^{2+}-ATPase isoform 4 (PMCA4) is the primary Ca^{2+} efflux pump in murine sperm, where it regulates motility. In *Pmca4* null sperm, motility loss results in infertility. We have shown that murine sperm PMCA4b interacts with Ca^{2+}/CaM-dependent serine kinase (CASK) in regulating Ca^{2+} homeostasis and motility. However, recent work indicated that the bovine PMCA4a splice variant (missing in testis) is epididymally expressed, along with 4b, and may be transferred to sperm. Here we show, via conventional and in situ RT-PCR, that both the splice variants of *Pmca4* mRNA are expressed in murine testis and throughout the epididymis. Immunofluorescence localized PMCA4a to the apical membrane of the epididymal epithelium, and Western analysis not only confirmed its presence but showed for the first time that PMCA4a and PMCA4b are secreted in the epididymal luminal fluid (ELF), from which epididymosomes containing PMCA4a were isolated. Flow cytometry indicated the presence of PMCA4a on mature caudal sperm where it was increased ~5-fold compared to caput sperm (detected by Western blotting) and ~2-fold after incubation in ELF, revealing in vitro uptake and implicating PMCA4a in epididymal sperm maturation. Coimmunoprecipitation using pan-PMCA4 antibodies, revealed that both variants associate with CASK, suggesting their presence in a complex. Because they have different kinetic properties for Ca^{2+} transport and different abilities to bind to CASK, our study suggests a mechanism for combining the functional attributes of both PMCA4 variants, leading to heightened efficiency of the pump in the maintenance of Ca^{2+} homeostasis, which is crucial for normal motility and male fertility.

calcium regulation, CASK, epididymis, epididymosomes, plasma membrane calcium pump, PMCA, sperm maturation

INTRODUCTION

When sperm leave the testis they are functionally incompetent, although morphologically mature. Functional maturity is gained as they traverse the epididymis, where they are in intimate and constant contact with secretions of the epithelial lining of the epididymis [1–3], the epididymal luminal fluid (ELF). During epididymal transit, which lasts ~5–10 days in mice [4], sperm acquire on their plasma membrane many molecular components from the ELF that aid in their maturation, in the absence of their own synthetic machinery [3, 5]. A large variety of proteins are added sequentially to sperm in the different regions of the epididymis, and many of these proteins are glycosyl phosphatidylinositol (GPI) linked and are readily added to the outer leaflet of the lipid bilayer of the sperm membrane [6, 7]. However, recently it has been shown that in humans and bulls, transmembrane proteins are also secreted in the ELF on epididymosomes, which are membranous vesicles known to transfer proteins to the sperm surface [8, 9].

Recent studies showed that an essential 10-pass transmembrane sperm protein, PMCA4, which is the major Ca^{2+} efflux pump in murine sperm [10], is synthesized in the rat [11] and bovine [12] epididymal epithelium. PMCA4 has the two major splice variants 4a and 4b, and 4b is thought to play a crucial role in Ca^{2+}clearance in murine sperm [10, 13] where deletion of *Pmca4* disrupts Ca^{2+} homeostasis and leads to loss of both progressive and hyperactivated sperm motility and ultimately to infertility [14, 15]. Interestingly, bovine sperm show a progressive switch from splice variant 4b in the upper to mainly 4a in the lower regions of the epididymal tract [12]. As sperm do not engage in new mRNA transcription or protein translation, this shift has been attributed to acquisition of PMCA4a from the ELF [12]. The switch from 4b to 4a is physiologically relevant because sperm face a steeper Ca^{2+} efflux requirement for hyperactivated motility in the female tract and PMCA4a has a higher basal activity and is more efficient than 4b in returning Ca^{2+} to resting levels [12, 16].

In light of these findings for testicular PMCA4 variants in bovine epididymis and sperm, we hypothesized that in the murine system, the PMCA4a variant may also be expressed in the epididymis and potentially secreted in the luminal fluid where it might be acquired by sperm during their epididymal transit and maturation. Our results reveal a difference in bovine and murine systems because we found that in mice, both *Pmca*4a and *Pmca*4b mRNAs are expressed in the testis and throughout the epididymis. Importantly, we show for the first time that PMCA4a is expressed in the ELF, is associated with epididymosomes, and is transferred from ELF to caudal sperm in vitro, suggesting that it plays a role in epididymal sperm maturation. Interestingly, in caudal sperm and in ELF both PMCA4a and PMCA4b variants could be coimmunoprecipitated with Ca^{2+}/CaM-dependent serine kinase (CASK), an interacting partner of PMCA4b that is known to play a role in signal transduction [13, 17], thus indicating that both of the Ca^{2+} pump variants function in a complex in sperm.

[1]Supported by National Institutes of Health grant NIH-RO3 HD061637 and the Delaware IDeA Networks of Biomedical Research Excellence (INBRE) Program to P.A.M.-D.
[2]Correspondence: Patricia A. Martin-DeLeon, Department of Biological Sciences, University of Delaware, Newark, DE 19716.
E-mail: pdeleon@udel.edu
[3]Co-first authors.

Received: 20 February 2013.
First decision: 8 April 2013.
Accepted: 15 May 2013.

eISSN: 1529-7268 http://www.biolreprod.org
ISSN: 0006-3363

MATERIALS AND METHODS

Animals and Reagents

Sexually mature 3- to 6-month-old male outbred mice (ICR and C57BL/6 strains; Harlan, Indianapolis, IN) were used throughout the investigation. In addition to these wild-type (WT) mice, *Pmca4* null mice were used to provide ELF for the coimmunoprecipitation (co-IP) assays. These mice were a generous gift from Dr. Gary Shull in whose laboratory they were generated [14]. Breeding and genotyping of these mice were described previously [14]. Studies were approved by the Institutional Animal Care and Use Committee at the University of Delaware and were in agreement with the *Guide for the Care and Use of Laboratory Animals published by the National Research Council of the National Academies, eighth ed., Washington, D.C*. All reagents and chemicals were of molecular biology grade and were purchased from Fisher Scientific Co., Sigma-Aldrich, or Invitrogen, unless otherwise specified.

Antibodies

Affinity purified goat polyclonal pan-PMCA4 antibody (Y20, sc 22080) raised against the N terminus of the rat protein and anti-human heat shock cognate protein 70 (HSC70; sc7298) mouse monoclonal antibody were purchased from Santa Cruz Biotechnology. A rabbit polyclonal β-actin antibody was obtained from Cell Signaling. Rabbit polyclonal antibodies against peptides specific for rat or bovine PMCA4a were generated and previously validated [12, 18]. As sequence analysis suggested a high probability of cross-reactivity with the mouse PMCA4a, these antibodies were used in our Western blot, immunofluorescence, and flow cytometric studies, all of which demonstrated that the antibodies were competent to specifically detect mouse PMCA4a. Anti-rat CASK/Ln2 mouse monoclonal antibody (#75-000), which cross-reacts with the mouse protein, was obtained from University of California at Davis, the National Institute for Neurological Disorders and Stroke, the National Institute for Mental Health (UC Davis/NINDS/NIMH) NeuroMab Facility. Secondary antibodies were purchased from Santa Cruz Biotechnology or Molecular Probes Inc.

Collection of Tissues, Epididymal Luminal Fluid, and Sperm

For in situ RT-PCR, the testes and three epididymal regions were snap-frozen in 2-methyl-butane (isopentane). For conventional RT-PCR and Western blotting, tissues, sperm, and ELF were collected as previously described [19–23]. Briefly, immediately after mice were CO_2 asphyxiated, epididymal regions were removed and placed separately in 300 μl of PBS with Complete protease inhibitor (Roche Diagnostics). The epididymal regions were finely minced and incubated for 10 min at 37°C to allow sperm to swim out. Tissue fragments were then separated from the sperm suspension by gravity settling, and the suspension was centrifuged (500 × *g* for 15 min at room temperature [RT]) to pellet the sperm. The resulting fluid was further clarified via centrifugation (16 100 × *g* for 20 min at 4°C) with the supernatant yielding ELF.

The tissue fragments were washed three times with 500 μl of PBS to release as many sperm as possible, and the suspensions were added to the sperm pellet to increase its size after further centrifugation (500 × *g* for 15 min). The final pellet was then washed with PBS before using for immunofluorescence or protein extraction, while tissue fragments were snap-frozen for conventional RT-PCR or stored at −80°C for protein extraction. The last procedure was performed using a solubilization buffer (62.5 mM Tris-HCl, 10% glycerol, 1% SDS, pH 6.8) with protease inhibitor, in which sperm and tissues were homogenized using a mortar and pestle. The homogenate was left overnight at 4°C before centrifugation (14 000 × *g* at 4°C for 15 min) to recover the supernatant. Protein concentrations in the supernatant and the ELF were measured using a bicinchoninic acid (BCA) assay kit (Pierce).

RNA Isolation and RT-PCR

Total RNAs from frozen testes and sperm-free epididymal tissues from two males were extracted using RNeasy mini kit (Qiagen), according to the manufacturer's directions. First-strand cDNA synthesis was performed with total RNA (1000 ng) in a 20-μl reaction volume, using random primers and the High Capacity RT kit with RNase inhibitor (Applied Biosystems) according to the manufacturer's instructions. To amplify cDNA samples, PCR reactions (25 μl final volume) were performed with 2 μl of cDNA for 30 cycles (Veriti thermocycler; Applied Biosystems), using the primers listed in Table 1. Negative controls (N) were set up in the absence of cDNA. Conditions of amplification of the samples and β-actin, an internal control, were an initial denaturation step of 5 min at 96°C, followed by 30 cycles of 30 sec at 96°C, 30 sec at 59°C, 1 min at 72°C, and a final extension of 5 min at 72°C. The PCR products (10 μl) were run in a 2% Nusieve agarose gel (Lonza, MD) in TAE (40 mM Tris-acetate, 2 mM EDTA, pH 8.5) containing ethidium bromide (10 μg/ml), along with a 100-bp ladder (Invitrogen). Amplicons were gel purified, and their identities were verified by DNA automated sequencing.

In situ RT-PCR tissue fixation and sectioning. Snap-frozen testes and epididymides from three males were thawed in RNA*later*-ICE (Ambion/Life Technologies) and fixed overnight in 4% paraformaldehyde. Samples were routinely processed (manually under RNase-free conditions) through graded alcohols and xylene and infiltrated with Paraplast X-tra (Leica). The samples were blocked, cut at a thickness of 5 μm on an RM2255 microtome (Leica) and floated from RNase-free water onto Probe-On Plus slides (Thermo Fisher). The tissue sections were heat immobilized at 60°C, deparaffinized, and rehydrated on a DRS 601 stainer (Sakura Fintek USA Inc.).

Direct in situ reverse transcriptase reaction. This assay was performed as described previously [24, 25] with modifications, by using GeneAmp in situ system 1000 (Perkin-Elmer). Tissue sections were overlaid with 50 μl of a master mixture consisting of diethylpyrocarbonate (DEPC) water, 5× EZ buffer, deoxyribonucleotide triphosphates, recombinant thermus thermophilus, and 25 mM $Mn(OAc)_2$ (Life Technologies) and covered with AmpliCover disks (Perkin-Elmer). Using a hot start ramp to 94°C for 1 sec, sections were incubated at 60°C for 45 min, followed by incubation at 4°C for 5 min.

PCR. Amplification of cDNA was performed using 10 μM of the primer detecting both the splice variants *a* and *b* in Table 1 (exon 19-F2, exon 21-R2). Sections were preincubated at 65°C for 1 min and then 35 cycles were performed at 94°C for 15 sec and 60°C for 30 sec, ending with a final incubation at 60°C for 7 min. PCR was completed in a 4°C soak/hold cycle. Subsequently the sections were washed in several changes of DEPC water, refixed in 100% ethanol, and very briefly air-dried.

PCR in situ hybridization. A biotinylated oligonucleotide probe (5′-/5Biosg/CAG TTT GAC GAC TCT-3′; Integrated DNA Technologies) hybridizing with a common sequence (nucleotides 3667–3681 in variant a and 3486–3500 in b) in the RT-PCR products was used. Sections were permeabilized in a 1:8 dilution of trypsin (Digest all kit, Cat. no. 00-3006; Invitrogen) and placed in a prehybridization buffer of formamide (50%), Denhardt solution (5×), dextran sulfate (10%), heparin (20 U/ml), and SDS (0.01%) and a salt solution containing 4M NaCl, 100 mM EDTA, 200 mM Trizma base, 100 mM NaH_2PO_4, and 100 mM Na_2HPO_4. Using capillary gap technology (MicroProbe system; Thermo Fisher), samples were denatured at 94°C for 5 min. Fresh hybridization buffer with the probe (10 μM) in a volume of 100 μl was placed on each slide and the temperature was dropped to 75°C for 5 min and 55°C for 1 h, followed by four stringent washes of 5 min each. Control slides were incubated in the hybridization buffer without the probe.

Sections were then blocked in 5% BSA in PBS for 1 h and washed in PBS. Hydrogen peroxide block was applied to quench peroxide activity, and detection was completed with GenPoint tyramide signal amplification system for biotinylated probes (DAKO). All slides were counterstained with Mayer hematoxylin and dehydrated, cleared, and mounted in Permount (Thermo Fisher) before microscopy.

TABLE 1. Primer pairs and product sizes.

Gene	GenBank accession no.	Variant	Region	Sequence	Size (bp)
Pmca4	NM_001167949	*a*	Exon 18 F-1	5′-GCA CTG GAT GTG GTG TCT CTT TAT-3′	417
	NM_001167949	*a*	Exon 20 R-1	5′-CAC TCA CTG CCC ACA GGA GGA-3′	417
		a	Exon 19 F-2	5′-GGA CGA GAT TGA CCT TGC CG-3′	469
	NM_213616.3	*b*	Exon 21 R-2	5′-CAC CAT CCA ACA GGA GCA CAC T-3′	278
β-actin			F-1	5′-CGT CGA CAA CGG CTC CGC CAT C-3′	100
			R-1	5′-CCA CCA TCA CAC CCT GGT GCC TAG G-3′	100

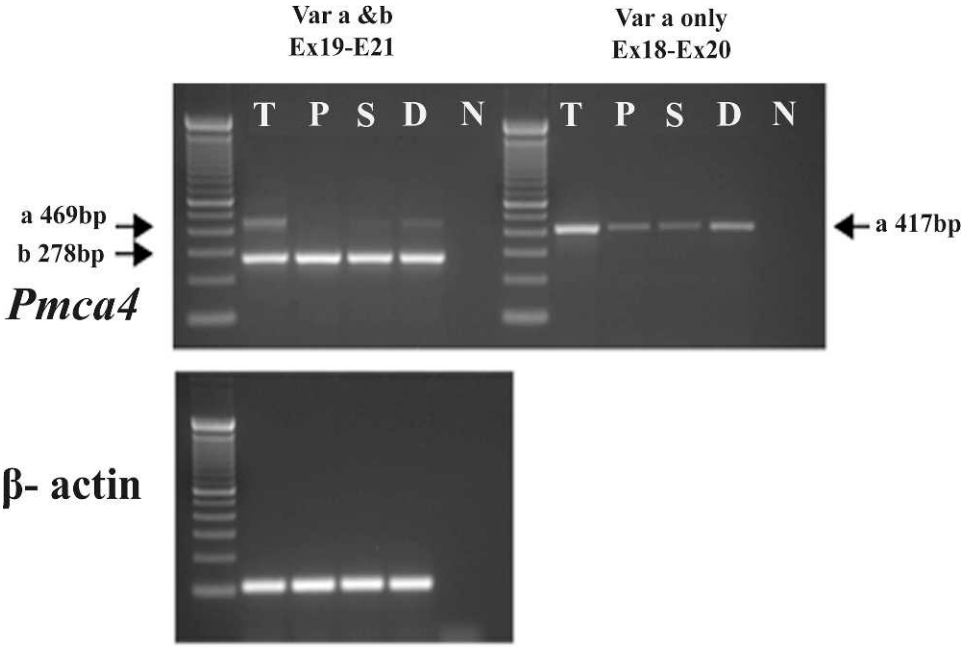

FIG. 1. Semiquantitative analysis of *Pmca4a* and *Pmca4b* mRNA via RT-PCR in murine testis (T) and epididymal tissues, as indicated (P = caput, S = corpus, and D = cauda). Negative control (N) was performed in the absence of cDNA. Products of primers amplifying both *Pmca4a* and *Pmca4b* transcripts are shown on the left, whereas only variant *4a* is detected in the panel on the right. The β-*actin* mRNA was used as an internal control. A 100-bp ladder was run in the left lane of each panel.

Immunofluorescence

Mouse testes and epididymides from four males were collected after euthanasia and immediately embedded in OCT (Tissue Tek) and frozen at −80°C. Cryostat sections (20-μm) were kept at −80°C until processing. Slides were fixed in an acetone:methanol solution at a ratio of 1:1, prechilled for 20 min at −20°C, and then allowed to air-dry for 10 min before being placed in protein blocker (1% BSA in PBS) for 1–2 h at RT. They were then incubated overnight at 4°C with the anti-PMCA4a primary antibody diluted at 1:50 in blocking solution, followed by washing with PBS (2×, 20 min). Sections were then incubated for 1 h at RT with Alexa Fluor 568-conjugated goat anti-rabbit immunogobulin G (IgG; 1:200 dilution; Molecular Probes) containing Draq-5,

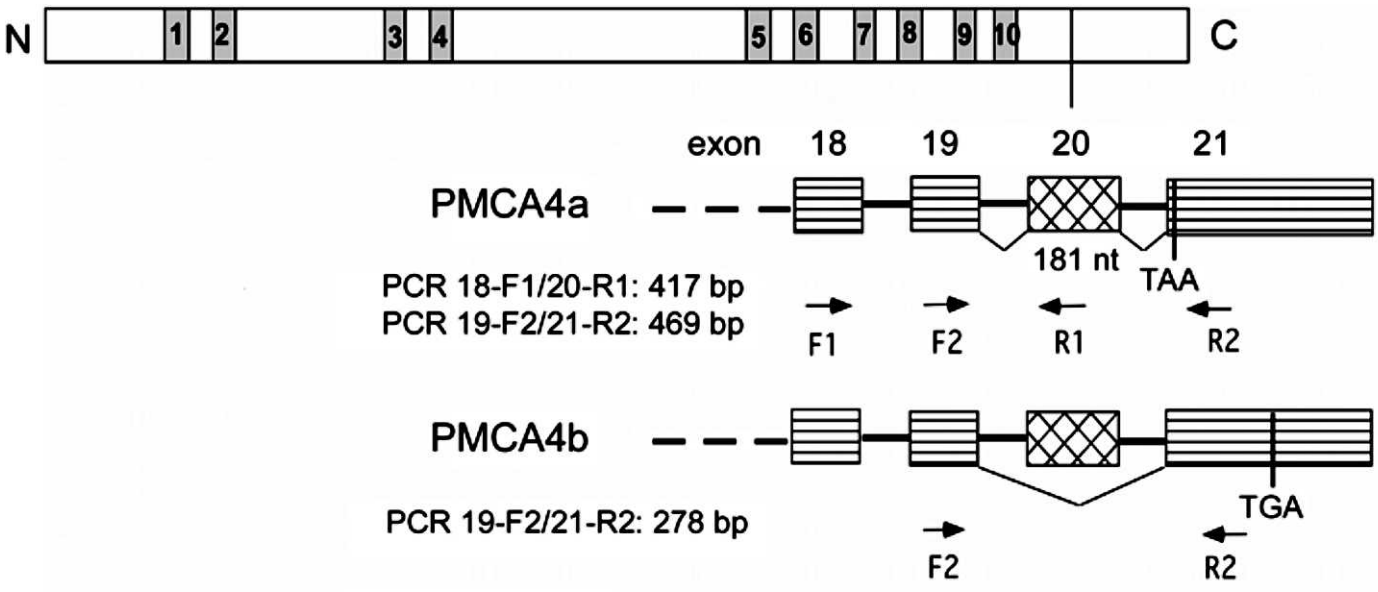

FIG. 2. Scheme of alternative splicing leading to PMCA4a and PMCA4b. A linear model of the PMCA is shown on top; the 10 membrane-spanning regions are numbered and the N and C termini are labeled. The site in the C-terminal tail where inclusion or exclusion of the alternatively spliced 181 nucleotide exon 20 results in PMCA4a and PMCA4b, respectively, is also indicated. The partial exon-intron structure of the mouse *Pmca4* (*Atp2b4*) gene from exon 18 to 21 is shown on the bottom, and the alternative splices resulting in PMCA4a and PMCA4b are indicated. The location of the stop codons (TAA and TGA) in PMCA4a and PMCA4b mRNA is also shown. The position of PCR primers used for detection of PMCA4a and PMCA4b transcripts (Table 1) is schematically indicated, and the expected sizes of the PCR products are given in base pairs.

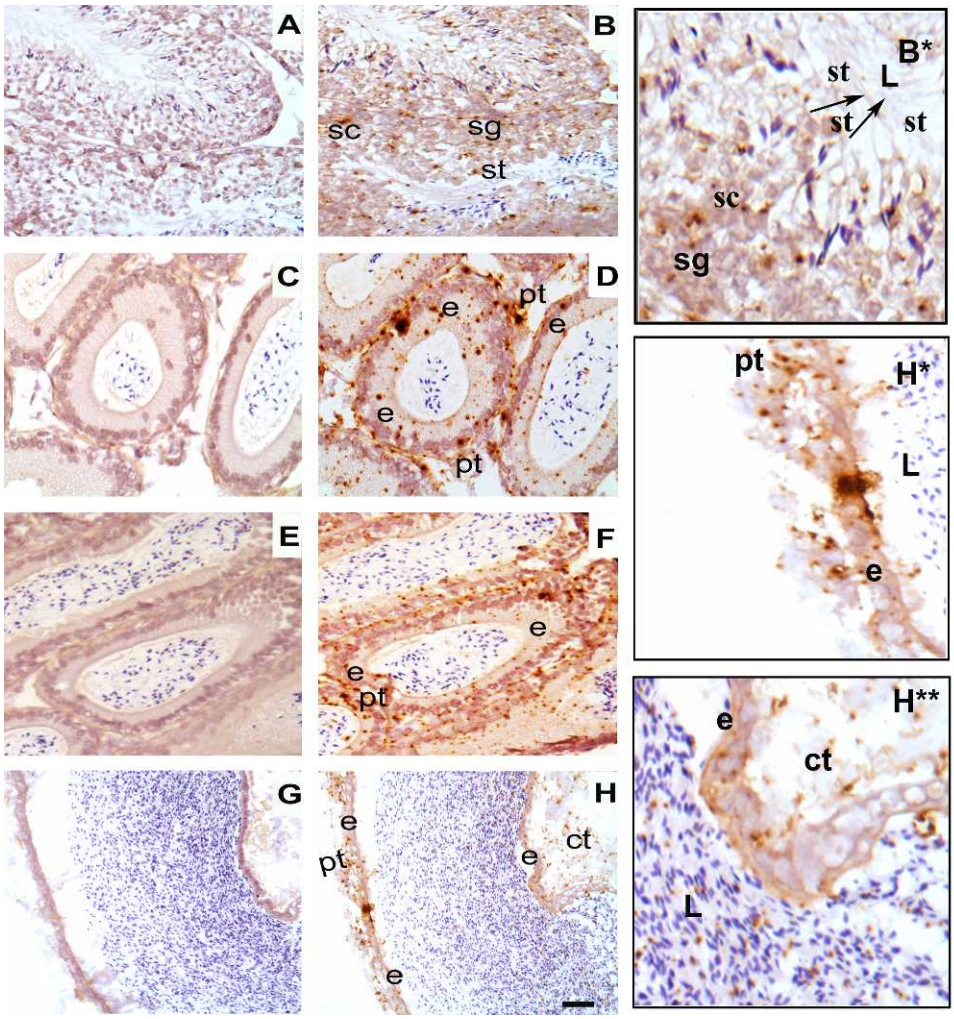

FIG. 3. In situ RT-PCR detects *Pmca4* transcripts in testis and epididymis. Primers 19 F-2 and 21 R2 (Table 1) were used for PCR, and detection was by a biotinylated oligonucleotide probe recognizing both 4a and 4b transcripts, as described in *Materials and Methods*. Negative controls (**A**, **C**, **E**, **G**) lacking the biotinylated detection probe showed no brown punctuate staining seen after probe hybridization. In the seminiferous tubule of the testis (**B**, **B***), spermatogonia (sg), spermatocytes (sc), and spermatids (st) are stained in a punctuate manner, indicating expression of *Pmca4* transcripts in all germ cell types. **B*** shows an enlarged section of the seminiferous tubule in which germ cell types are identifiable. **D**, **F**, **H**) (**H*** and **H**** show enlargements) show staining in the caput, corpus, and cauda, respectively; where the epithelial cells (e) are stained as well as the peritubular cells (pt). In the cauda transcripts are also detected in connective tissue (ct) around the tubules and are absent from sperm in the lumen (L). Bar = 25 μm.

1:2000 dilution, as a nuclear stain (Biostatus Ltd.), followed by washing with PBS (2×, 20 min). Finally, the samples were mounted with mounting medium and coverslipped. Slides were visualized using an LSM780 model confocal microscope (Carl Zeiss) with a plan apochromatic 20× objective. Negative control samples were incubated with rabbit IgG instead of the primary antibody.

SDS-PAGE and Western Blot Analysis

Western blotting of total protein extracts and ELF was performed as previously described [26, 27] using WesternBreeze chemiluminescent immunodetection kit (Invitrogen) according to the manufacturer's instructions. Proteins (20–60 μg) were fractionated by SDS-PAGE under reducing conditions (after heating the samples at 37°C for 10 min in the presence of 100 mM dithiothreitol) on 10% or 12% polyacrylamide gels and transferred onto nitrocellulose membranes, according to standard protocols. After blocking, membranes were probed with anti-PMCA4a primary antibody (rat, 1:500 dilution; bovine, 1:200 dilution) overnight, and proteins were visualized using alkaline phosphatase (AP)-conjugated secondary antibodies and reagents from the Western blotting detection kit. The actual amounts of proteins loaded on the gels were assessed after stripping the membrane (Restore Western blot stripping buffer; Thermo Scientific) and reprobing with β-actin antibodies (1:2000), a housekeeping protein or HSC70 (1:1000), and the appropriate AP-conjugated secondary antibody. Protein bands were analyzed by densitometry (FluorChem 8800; Alpha Innotech Corp.), and the ratio of PMCA4a to the loading controls was determined and plotted.

Fractionation of Epididymal Luminal Fluid

Clarified ELF was obtained as described above from six males. Using an Optima L-70 centrifuge with a Ti60 rotor (Beckman), the ELF was subjected to ultracentrifugation at 120 000 × *g* for 2 h at 4°C, as previously reported from our laboratory [22], to separate the soluble (supernatant) from insoluble fraction. The proteins from the supernatant were precipitated with 3 volumes of acetone, recovered in sample buffer, and subjected to Western blotting as described previously [27], along with the pellet that was also resuspended in the buffer.

Flow Cytometric Analysis of PMCA4a in Sperm

To confirm the Western blot data for the presence of PMCA4a in sperm, immunofluorescence was performed using a modification of the procedure published earlier [26]. Briefly, freshly recovered caudal sperm from two to three males per experiment were washed in PBS and fixed with 1.5% paraformaldehyde at RT for 1 h and then washed twice with PBS, permeabilized (0.1% Triton X-100 in PBS) at RT for 10 min, washed with blocking buffer (2% BSA in PBS), and incubated in blocking buffer at RT for 30 min. The cells were incubated in PMCA4a primary antibody (rabbit anti-rat,

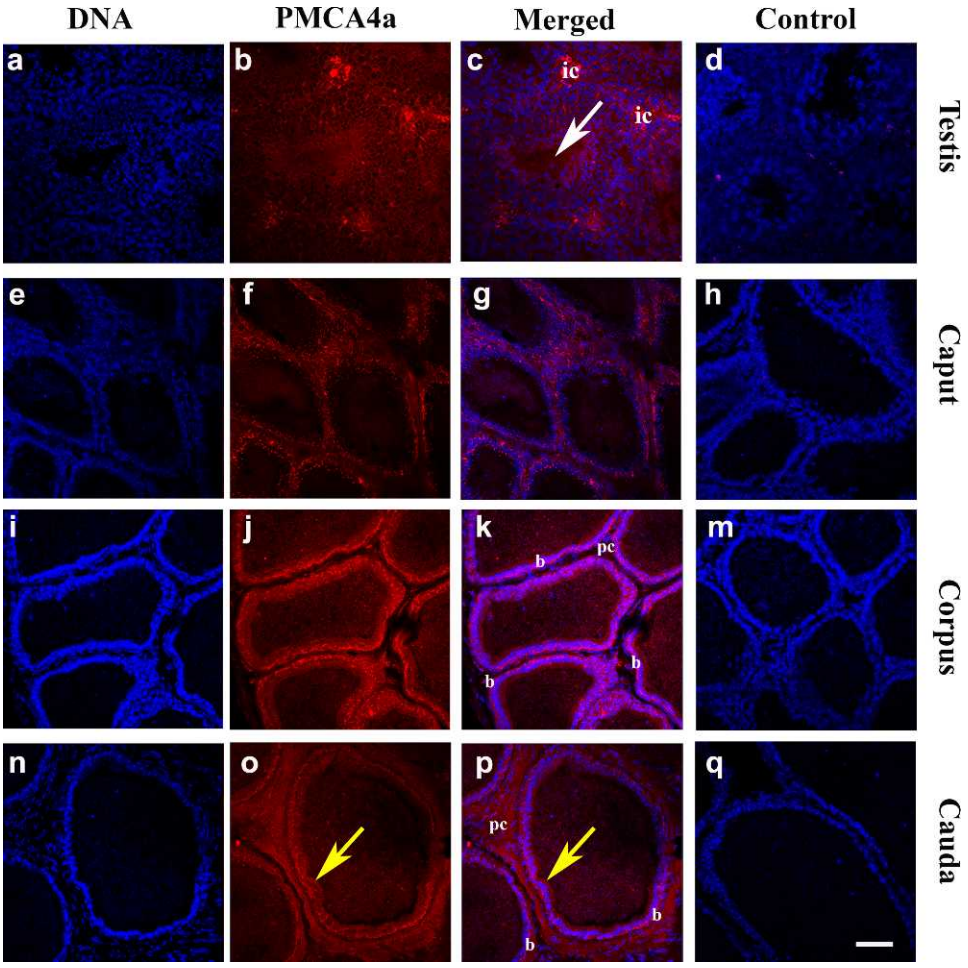

FIG. 4. Immunolocalization of PMCA4a in testis and epididymis, using a rabbit polyclonal anti-rat PMCA4a antibody. Indirect immunofluorescence was performed with frozen sections of murine testis (**a**–**c**), caput epididymis (**e**–**g**), corpus epididymis (**i**–**k**), and cauda epididymis (**n**–**p**). In the testis PMCA4a staining (red) was detected in the interstitial cells (ic) between the seminiferous tubules as well as within germ cells in the tubules where it could be seen in the lumen (white arrow) where sperm reside. In epididymal tissues staining was weakest in the caput epididymis. In the corpus and cauda epididymides strong PMCA4a staining was detected at the basement lining (b) of the epithelial cells and the peritubular cells (pc); staining was also detected at the apical surface of the epithelial layers of these tissues. Staining was moderate in the apical lining of the cauda and the lumen (yellow arrow). The nuclei were visualized by staining with Draq-5 (blue). Negative controls using IgG (**d**, **h**, **m**, **q**) are seen for testis, caput, corpus, cauda, respectively. The images were captured using confocal microscopy with a 20× objective lens (plan apochromatic). Bar = 70 μm (same scale for all photomicrographs).

1:400) or rabbit IgG (nonspecific) for the control at RT for 1 h and then washed 3× with PBS and incubated in the appropriate secondary fluorescein isothiocyanate-conjugated antibody at RT for 30 min. Sperm pellets were then washed 3× with PBS and resuspended in 1–1.5 ml of PBS for analysis, using a FACSCalibur unit (Becton Dickinson) flow cytometer equipped with an argon laser at 488 nm excitation.

Sperm Uptake of PMCA4a In Vitro

Caudal sperm collected from 2–3 sexually mature mice as described previously [22] were incubated in ELF recovered in PBS containing 2 μM zinc acetate, pH 5.5, and protease inhibitor and clarified [22] after being subjected to centrifugation at 3500 × *g* for 20 min. This PBS vehicle for the ELF was used for control samples. After 30 min of incubation at 37°C, control and test samples in ELF were washed with PBS and treated with rabbit anti-rat PMCA4a antibody (1:200 dilution) at RT for 1 h. Sperm were washed 3× with PBS and incubated in secondary antibody (Alexa Fluor- 488-conjugated donkey anti-rabbit IgG [1:200]) for 30 min). Sperm were then washed 3X with PBS and subjected to flow cytometric analysis, using a FACSCalibur (Becton Dickinson) as described above.

Coimmunoprecipitation

PureProteome protein G magnetic beads (Millipore Corp.) were washed twice in PBS with 0.1% Tween 20 and recovered by centrifugation at 2500 × *g* for 5 min. The beads were then resuspended in 100 μl of PBS with 2 μg of anti-CASK antibodies for 2 h at 4°C. After incubation, the beads were centrifuged at 2500 × *g* for 5 min and washed twice in PBS. The beads were then resuspended in 500 μl of ELF (protein concentration of 1 mg/ml) pooled from all three epididymal regions of WT or *Pmca4* null mice, which were used as a control. In some experiments beads were incubated in sperm protein extracts as previously described [26]. Following incubation in ELF for 16 h at 4°C, the beads were centrifuged at 2500 × *g* for 5 min and washed twice with PBS. The protein bound was solubilized in sample buffer, analyzed by SDS-PAGE, and electrotransferred to nitrocellulose membranes. Coimmunoprecipitated PMCA4 was detected using goat pan-PMCA4 polyclonal antibody (1:500 dilution) and the Western Breeze chemiluminescent immunodetection kit mentioned above. After visualizing the PMCA4 bands, the membranes were stripped and reprobed with anti-CASK antibodies (1:1000 dilution).

Statistical Analysis

All experiments were performed at least three times. Data were analyzed using Image J software. One-way ANOVA was performed with the means ± SEM to detect statistical significance. Differences were considered significant at $P < 0.05$.

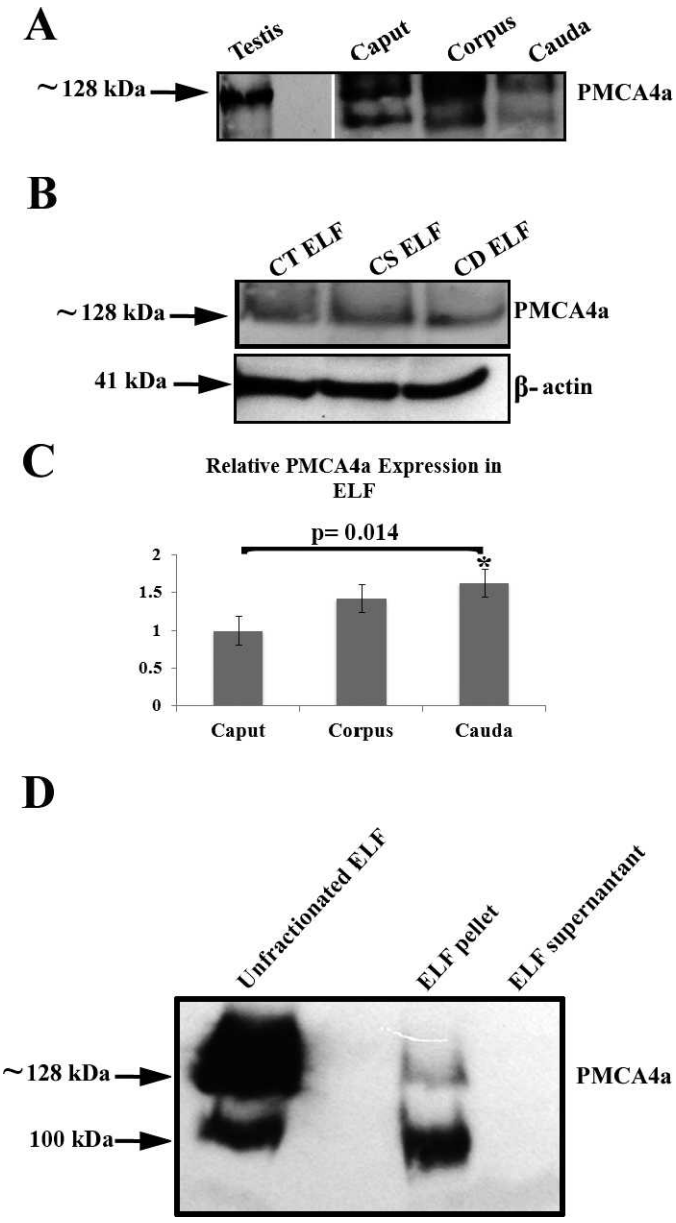

FIG. 5. Western blot analysis of PMCA4a expression in murine testis and epididymal tissue (**A**) and ELF (**B**, **D**). Twenty and 45 μg of protein/lane were loaded in **A** and **B**, respectively. PMCA4a was detected using a rabbit polyclonal anti-bovine PMCA4a antibody (1:175 dilution) in **A**, and a rabbit polyclonal anti-rat PMCA4a antibody (1:500 dilution) in **B**. **A** shows the presence of PMCA4a in the testis and all three epididymal regions, while **B** shows PMCA4a in purified ELF from each of the three epididymal regions. Blots of the latter were stripped and reprobed for β-actin as a loading control, and PMCA4a band intensities were analyzed by densitometry using Image J software. The relative expression in corpus/cauda compared to the caput is displayed in a bar graph in **C**. Values are expressed as means ± SD (n = 3), with expression highest in the cauda (*P = 0.014 versus caput). **D** shows immunoblotting of proteins from pellet and supernatant fractions of equivalent volumes of ELF, following ultracentrifugation. PMCA4a, seen in the pellet, is absent from the supernatant. An immunopositive band (100 kDa) which is also seen in **A** is of unknown origin, but most likely a breakdown product as it is much fainter in the unprocessed ELF and is not seen in **B**.

RESULTS

Pmca4 *Transcript Splice Variants in Testis and Epididymis Are Differentially Expressed*

As shown in Figure 1, RT-PCR primers used to detect *Pmca4* transcripts (Table 1), amplified products of the expected sizes in all three regions of the epididymis. Using β-actin as an internal control for semiquantitative analysis, *Pmca4b* is expressed evenly throughout the caput (P), corpus (S), and cauda (D) and at similar levels as in the testis (positive control). In contrast, variant *4a* is differentially expressed with the strongest expression in the testis and with increasing levels from the caput to the cauda, as determined by two different primer pairs (Fig. 2, see scheme).

The localization of *Pmca4* transcripts in the different cell types in the testis, caput, corpus, and cauda was analyzed using in situ RT-PCR (Fig. 3). Controls without signal are seen in Figure 3, A, C, E, and G. In the testis (Fig. 3B), expression of the transcripts is seen in spermatogonia, spermatocytes, and spermatids in the seminiferous tubules. In the epididymis, the mRNA is localized to the epithelial lining of all three regions and is also seen in the peritubular cells (Fig. 3, D, F, and H), as well as in the connective tissue surrounding the tubules (Fig. 3H).

Immunodetection of PMCA4a in Testis, Epididymis, ELF, Epididymosomes, and Sperm

Consistent with the mRNA expression data, immunofluorescence revealed the presence of PMCA4a in all germ cell stages in the testis (Fig. 4, b and c). There was positive immunoreactivity in the lumen of the seminiferous tubules, where sperm reside (Fig. 4c, arrow). The three epididymal regions were positively stained, with the lowest intensity in the caput (Fig. 4, f and g). Positive PMCA4a staining was detected in the apical surface of the epithelial lining of the corpus and cauda, next to the lumen, and in the lumen (Fig. 4, j and k and o and p). It could also be seen in the peritubular cells. Immunostaining was absent in the negative controls, where IgG was used in place of the primary antibody (Fig. 4, d, h, m, and q).

Western blotting was performed to confirm the immunofluorescence findings. Figure 5A shows the presence of the ~128-kDa PMCA4a band in protein extracts from the testis (positive control) and all three epididymal regions. Figure 5B shows the presence of PMCA4a in clarified ELF from all epididymal regions where the cauda showed the highest and the caput the lowest amounts of PMCA4a expression, as revealed by the β-actin loading control (Fig. 5C). Thus, there was a tendency for an increase in PMCA4a from the proximal to the distal end of the duct. When ELF was fractionated by ultracentrifugation, Western blotting revealed that 100% of the PMCA4a was associated with the insoluble fraction or the epididymosomes (Fig. 5D).

To localize PMCA4a on the surface of mature caudal sperm and to confirm its presence in sperm, flow cytometry and Western blotting were used. Flow cytometry displayed ~10-fold difference in fluorescence intensity between caudal sperm treated with anti-PMCA4a primary antibody and that of the IgG control, confirming the specificity of the antibody and the presence of PMCA4a on murine sperm (Fig. 6A). In addition to confirming PMCA4a as a sperm protein, Western blotting (Fig. 6B) revealed that caudal sperm have significantly ($P = 0.003$) elevated levels compared to caput sperm, where PMCA4a levels are ~5-fold lower, as revealed by densitometry (Fig. 6C).

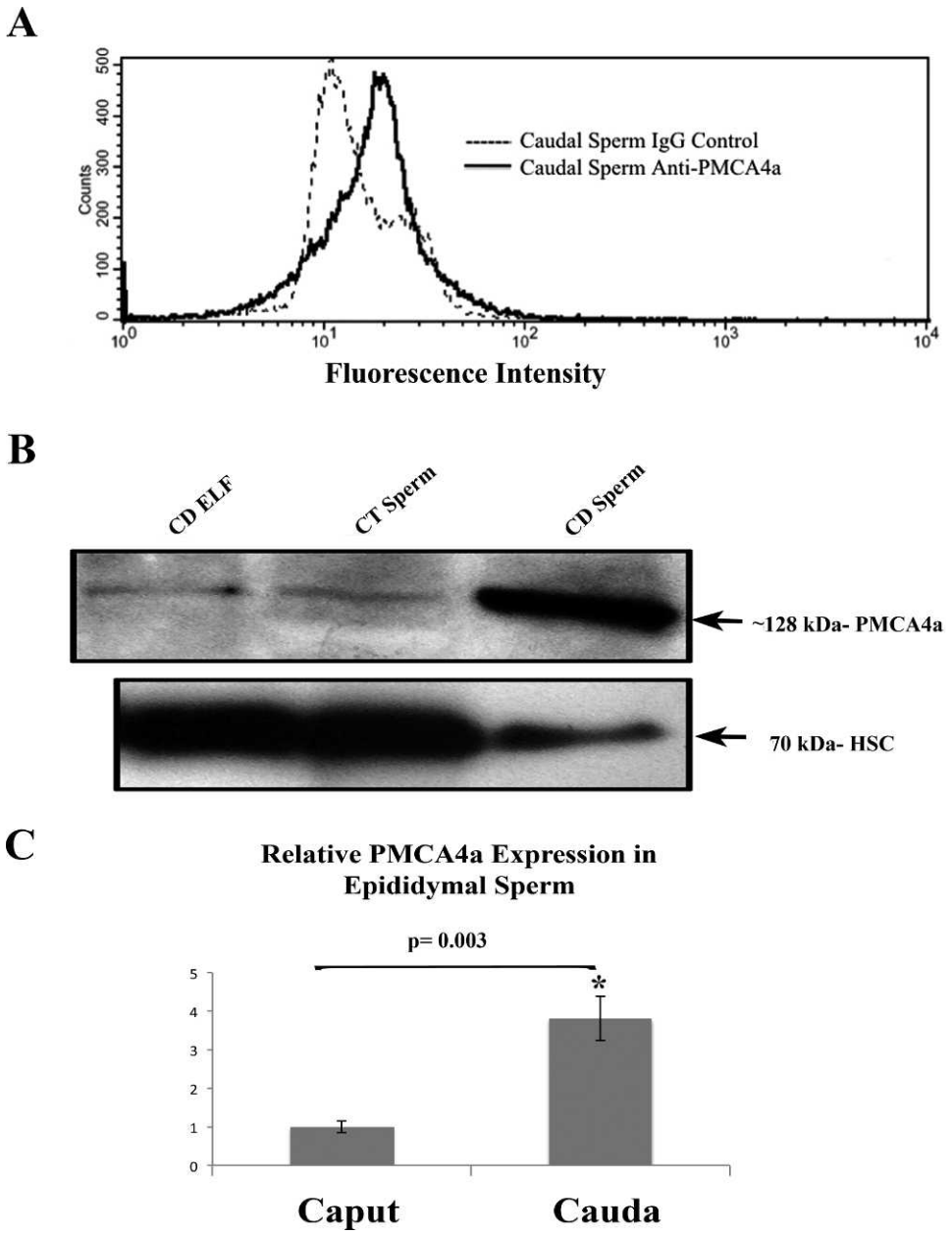

FIG. 6. Flow cytometry and Western blot analyses reveal the presence of PMCA4a in murine caudal sperm. **A**) Quantitative immunofluorescence analysis of 50 000 cells treated with the rabbit polyclonal anti-bovine PMCA4a primary antibody (1:20 dilution) shows a marked right shift of the peak, indicating increased fluorescence intensity (~10-fold) compared to the controls, which were treated with rabbit IgG for flow cytometry. **B**) Western blotting using anti-rat PMCA4a primary antibody (1:400 dilution) shows significantly more PMCA4a in caudal (CD) than caput (CT) sperm. The blot was stripped and reprobed for HSC-70 (70 kDa) as a loading control. The left lane shows the presence of PMCA4a in caudal ELF. **C**) Densitometric analysis of the blots was performed, using Image J software, to determine relative expression of PMCA4a in caput and caudal sperm. The bar graph shows a ~5-fold increase in the latter; values are expressed as means ± SD (n = 3). *$P = 0.003$.

Caudal Sperm Acquire PMCA4a from the Epididymal Luminal Fluid

To determine whether the accumulation of PMCA4a in mature sperm might be caused by uptake from the ELF, we incubated washed caudal live sperm in purified ELF or in PBS, as a control, under physiologically relevant conditions of temperature, pH, and the presence of zinc [28]. Quantitative immunofluorescence analysis of 50 000 sperm by flow cytometry showed a remarkable ~2-fold increase in PMCA4a in caudal sperm incubated for 30 min in ELF compared to sperm kept in control PBS (Fig. 7). Although the epitope for anti-PMCA4a antibody is on the cytosolic side of the membrane, evidence that it can be accessed by the antibody is seen from the finding that a proportion of epididymosomes retain uranyl acetate that is used for their negative staining [22]. Thus, the results provide direct evidence for the uptake of PMCA4a into mature sperm from the ELF and help explain the increased expression of PMCA4a in caudal sperm, which are known to be transcriptionally inactive.

Co-IP Assays Reveal PMCA4a and PMCA4b Coexist in a Complex with CASK

Recently it was shown in murine sperm that PMCA4 colocalizes on the principal piece of the sperm flagellum with

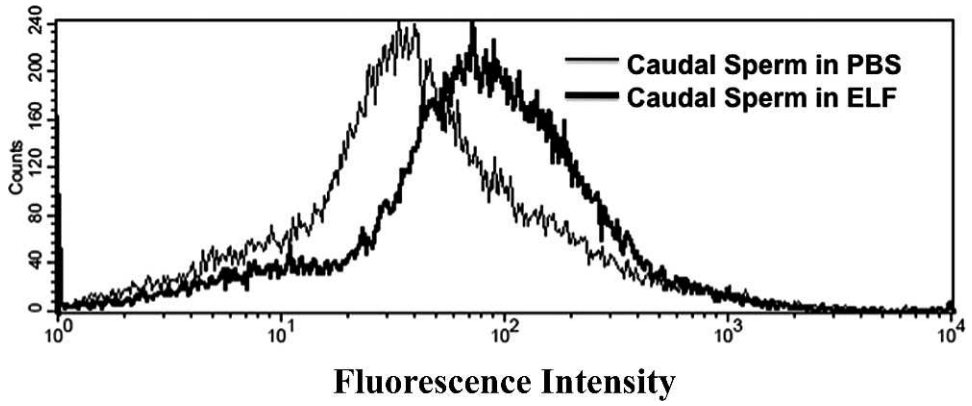

FIG. 7. Flow cytometric analysis of PMCA4a uptake into caudal sperm incubated in ELF combined from all three regions of the epididymis. Caudal sperm were incubated for 30 min at 37°C in PBS or ELF. Quantitative immunofluorescence analysis of 50 000 sperm/group by flow cytometry shows a 2-fold increase of PMCA4a after incubation in ELF compared to control (PBS). The graph is representative of experiments done in duplicate.

CASK, a signaling protein to which PMCA4b binds via its PSD-95/Dlg/ZO-1 (PDZ) ligand at the C terminus [26]. To gain insights into the functioning of PMCA4a in relation to PMCA4b, we performed co-IP assays using anti-CASK antibodies on ELF, as well as sperm lysate. Using pan-PMCA4 antibody for the Western blot in four replicated experiments, we found that PDZ domain-bearing CASK, in addition to immunoprecipitating PMCA4b, also coimmunoprecipitated PMCA4a in both sperm and in ELF. In Figure 8, ELF from WT but not from *Pmca4* KO males showed the ~133-kDa PMCA4b band clearly separated from the PMCA4a band (~128 kDa), which is smaller due to the truncated C-terminal tail encoded by the alternatively spliced exon 20 in the mRNA (Fig. 2). When the gels were stripped and reprobed with CASK antibodies, the total protein and the IPs showed the 60-kDa soluble CASK band (Fig. 8, lower panel), indicating that PMCA4a and PMCA4b are in a complex with CASK in the WT ELF. Interestingly, both the 60-kDa soluble CASK and the ~100-kDa insoluble CASK are present in the ELF total protein, with the latter being far more abundant.

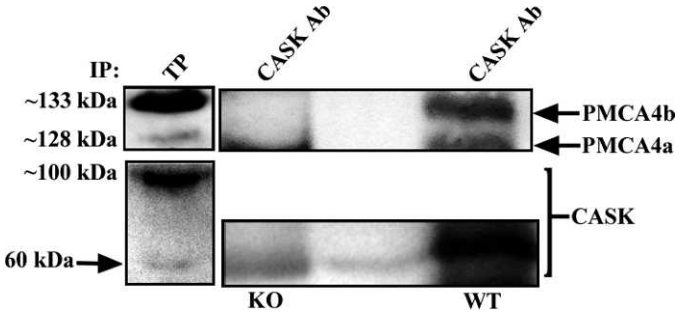

FIG. 8. Co-IP of PMCA4a and PMCA4b with CASK in epididymal luminal fluid (ELF). Both variants are seen in total protein (TP) in ELF pooled from all three epididymal regions in the Western blot and after subjecting the ELF to IP with anti-CASK antibodies. While the PMCA4 bands are seen in WT ELF, they are missing from ELF of *Pmca4* KO mice (negative control). As CASK cannot bind to PMCA4a and there is no PMCA4b in the KO samples [14], the band at ~128 kDa seen in this lane is nonspecific. The lower panel shows the blot after stripping and reprobing with anti-CASK antibodies. The 60-kDa CASK band is seen in the IP of WT and KO ELF as well as in the TP, which also showed the ~100-kDa insoluble CASK band in far more abundance. The faint 60-kDa band in the empty lane in the middle of the blot is a runover from the WT lane. The experiments were repeated at least four times.

DISCUSSION

PMCA4 Splice Variants Are Differentially Expressed in Testis and Epididymis and Are Transferred to Sperm from Epididymal Luminal Fluid

Gene transcripts of *PMCA* family members are known to undergo alternative splicing [29]. For *PMCA4*, splicing at the C terminus generates two major variants, 4a and 4b (Fig. 2), which display structural and functional differences [30, 31]. The two splice variants differ in their kinetics of calmodulin activation and their effectiveness in Ca^{2+} clearance, with 4a showing a higher basal activity and greater ability to rapidly return Ca^{2+} to resting levels [16, 32]. In the present study, we have characterized the expression and cellular distribution of these PMCA4 splice variants in the murine testis and epididymis. This is of particular interest because PMCA4 is the major calcium extrusion pump in sperm, and homozygous deletion of *Pmca4* results in male infertility and strikingly elevated Ca^{2+} levels [14, 15]. However, whether different PMCA4 splice variants are expressed in the testis and during spermatogenesis and how their relative abundance may change during sperm maturation have not yet been investigated. In contrast to the bovine testis, where RT-PCR revealed only 4b mRNA [12], the murine testis expresses the transcripts for both variants, although our semiquantitative analysis indicates that 4b is more abundant than 4a. The expression of both murine transcripts is consistent with earlier findings, using the less sensitive Northern blot assay [15], and also agrees with data reported in the rat [11].

Importantly, transcripts for the murine PMCA4a and PMCA4b isoforms are present in all germ cell stages (spermatogonia, primary and secondary spermatocytes, and spermatids), unlike those in the rat and bovine, where they are restricted to the earlier stages [11, 12]. It is unclear if this discrepancy is due to species differences or to the method of transcript detection. In the mouse, the highly sensitive in situ RT-PCR technique was used rather than the in situ transcript hybridization used in the other species [11, 12].

Our results reveal that the PMCA4 mRNA splice variants in the murine epididymis show markedly different levels and distribution of expression. Variant 4b was more abundant and was equally expressed in all three epididymal regions and in the testis. In contrast, 4a showed the highest expression in testis followed by the cauda and the smallest amount in the caput (Fig. 1). Although there may be species-specific differences in the distribution of 4a in the epididymis [11, 12], generally the

cauda (where sperm undergo their final maturation in the male and where they are stored [33]) appeared to have the highest expression of this mRNA splice variant.

The localization of PMCA4a protein in both the murine testis and epididymal regions paralleled that of the mRNA expression. Immunofluorescence revealed that all germ cell stages exhibit strong expression of the protein. In the epididymal regions, the protein was detected in the peritubular cells and in the epithelium where expression was seen in the apical regions lining the lumen. This finding parallels that seen in the bovine epididymis [12] but deviates from data in the rat, where PMCA4 appeared to be localized only in the basolateral membranes of the principal and basal cells of the caput epididymal epithelium [11]. PMCA4a protein expression in the epididymis was confirmed by Western blotting that detected the ~128-kDa band in all tissues (Fig. 5A). The expression of murine PMCA4a in the apical plasma membranes of the epididymis strongly suggests that it is secreted into the lumen: PMCA concentrated in glandular epithelial cells in a variety of tissues is known to be secreted (e.g., into milk from the apical membrane of lactating mammary gland epithelia) [34–37]. Indeed, Western blots revealed that the ELF from each epididymal region contained the ~128-kDa PMCA4a variant (Fig. 5B) and that both 4a and 4b are present in the ELF pooled from all regions (Fig. 8).

As expected, the relative levels of PMCA4a in the ELF from the three regions mirrored those in the tissues. They increased from the proximal to the distal region, with the largest amount detected in caudal ELF where it was ~1.7-fold higher than in caput ELF. The distribution of PMCA4a in the epididymis correlates with that in previous studies, showing that the corpus/cauda junction plays a major role in sperm maturation [38, 39], although other studies implicate the distal caput in mice [40, 41].

Secretion of epididymal proteins from the epididymal epithelium occurs through an apocrine pathway in which blebs (carrying membrane vesicles) dislodge from the apical membrane and enter the lumen, where they release membranous vesicles or epididymosomes [42]. These epididymosomes have been shown to carry membrane proteins that are then transferred to the sperm plasma membrane [43, 44]. Our study shows for the first time that murine epididymosomes (Fig. 5D) carry PMCA4a, a 10-pass transmembrane protein. As expected, the soluble fraction of the ELF was devoid of the protein. Importantly, we found that incubation of sperm in unfractionated ELF increased sperm PMCA4a levels by ~2-fold after 30 min of co-incubation, consistent with the role of epididymosomes in PMCA4a transport.

PMCA4a and PMCA4b Are Involved in Sperm Maturation and Function

Devoid of transcriptional machinery, sperm progress toward functional maturity in the epididymis by the acquisition of proteins from the ELF during their transit [1–3]. Our data (Fig. 6B) show that as sperm transit the epididymis, they acquire PMCA4a, resulting in an ~5-fold increase in the level of PMCA4a in caudal sperm compared to caput sperm. This may help explain the 2- to 6-times lower concentration of cytosolic Ca^{2+} in caudal sperm than in caput sperm [45] and the gain of motility in the former where the potential for Ca^{2+} clearance is markedly increased. Secretion of PMCA4a in the ELF on epididymosomes (as detected by the presence of the pump in the ELF, specifically on the insoluble membranous vesicle fraction) provides the means by which this acquisition occurs. Epididymosomes are known to be the vehicles for protein transfer in the ELF [43, 44] and have been previously identified in the mouse [22, 46]. Because both PMCA4 splice variants are present in the ELF, it is highly likely that the 4b variant is also acquired by sperm during their maturation. The combination of PMCA4 splice variants in a certain ratio on the sperm surface is likely required to optimize the PMCA4-mediated Ca^{2+} regulation in sperm.

Why might the two splice variants need to be coexpressed in mature sperm? PMCA4a and PMCA4b differ in their regulation by calmodulin and phosphorylation, as well as in their abilities to engage in PDZ domain-mediated protein interactions with signaling and scaffolding proteins [29, 47]. Only the 4b variant contains a PDZ binding C-terminal sequence [29], which has been shown to interact with the PDZ domain containing CASK [26]. In mouse sperm, the PMCA4b/CASK interaction regulates Ca^{2+} handling in a manner dependent on the sperm membrane protein junctional adhesion molecule-A (JAM-A) [26]. Indeed, physical association of JAM-A and CASK has been demonstrated; and CASK, PMCA4b, and JAM-A have been localized on the proximal principal piece of the mouse sperm flagellum [26]. PMCA4a lacks the PDZ-binding C-terminal sequence and is thus unable to bind to CASK via this mechanism. This may render PMCA4a function CASK- and JAM-A-independent and allow this more efficient pump to handle increased demands on Ca^{2+} extrusion in response to rapid Ca^{2+} fluctuations in mature, hyperactivated motile sperm. Support for this notion is provided by the finding that although *Jam-A* null sperm have reduced hyperactivated motility, the extent of the reduction does not lead to sterility [48]. Interestingly, however, co-IP assays of sperm proteins revealed that at least some PMCA4a, together with PMCA4b, is intimately associated with CASK in a multiprotein complex [26]. It should be noted that although Aravindan et al. [26] did not comment on the presence of both PMCA4 variants in the complex with CASK, the data they presented clearly displayed both. The results in the present study are consistent with those data for sperm and extend the findings to ELF, where both PMCA4a and PMCA4b coimmunoprecipitated with CASK (Fig. 8).

The basis for the association of PMCA4a in a complex with CASK is unknown. However, it is possible that 4a and 4b may dimerize, as the pump can be activated by dimer (oligomer) formation through the C-terminal tail [49–51]. Hence, such a heterodimer could be associated with CASK through the PMCA4b-PDZ interaction. Also, alternatively, PMCA4a may be loosely associated in a complex with CASK, which is a scaffold protein that anchors other proteins to the cytoskeleton [52]. The association of the two variants in the complex detected here suggests a mechanism by which sperm can optimize the functions of PMCA4 Ca^{2+} transport and signal transduction. As mentioned above, PMCA4a is the more efficient variant with respect to Ca^{2+} efflux, but it lacks the PDZ domain-binding ligand [53] required for communication and signaling cross-talk. Association of 4a with 4b in a complex with CASK, a signaling protein, may allow both isoforms to receive signals from the cell and the environment. Selective KO of the PMCA4a splice variant in testis and sperm will be required to determine the specific role of this pump isoform compared to PMCA4b in sperm Ca^{2+} handling, motility, and fertility. Based on work showing the role of epididymosomes in the uptake of GPI-linked proteins by sperm [22], future studies will investigate the mechanism by which the PMCA4 variants are acquired by sperm during maturation in the ELF, as well as the impact of PMCA4a acquisition on sperm function.

This study shows that both splice variants of PMCA4 mRNA are present in the mouse testis and in all three epididymal regions, with variant 4b being more abundant and equally expressed in all tissues. We show for the first time that PMCA4 variants 4a and 4b are secreted in the ELF combined from all epididymal regions and that 4a is markedly increased on caudal versus caput sperm, consistent with its transfer from the ELF, through epididymosomes. Co-IP studies suggest that in epididymis and sperm, both variants reside in a complex with CASK, although only PMCA4b has a CASK PDZ-domain interacting motif. This association may provide a mechanism for combining the functional attributes of both PMCA4 variants, leading to a heightened efficiency of PMCA4-mediated Ca^{2+} handling in mouse sperm, where the maintenance of Ca^{2+} homeostasis is crucial for sperm motility and male fertility.

REFERENCES

1. Cooper TG. Role of the epididymis in mediating changes in the male gamete during maturation. Adv Exp Med Biol 1995; 377:87–101.
2. Jones RC. Membrane remodeling during sperm maturation in the epididymis. Oxf Rev Reprod Biol 1989; 11:285–337.
3. Jones RC. Plasma membrane structure and remodeling during sperm maturation in the epididymis. J Reprod Fertil Suppl 1998; 53:73–84.
4. Robaire B, Hinton BT, Orgebin-Crist M. The epididymis. In: Neill J, Plant T, Pfaff D, Challis J, Kretser D (eds.), Knobil and Neill's Physiology of Reproduction, vol. 1, 3rd ed. New York: Raven Press; 2006:1071–1148.
5. Cooper TC. Interactions between epididymal secretions and spermatozoa. J Reprod Fertil Suppl 1998; 53:119–136.
6. Kirchhoff C, Pera IL, Derr PG, Yeung CH, Cooper TG. The molecular biology of the sperm surface. Adv Exp Med Biol 1997; 424:221–232.
7. Kirchhoff C, Hale G. Cell-to-cell transfer of glycosylphosphatidylinositol-anchored membrane proteins during sperm maturation. Mol Hum Reprod 1996; 2:177–184.
8. Thimon V, Frenette G, Saez FJ, Thabet MT, Sullivan RM. Protein composition of human epididymosomes collected during surgical vasectomy reversal: a proteomic and genomic approach. Hum Reprod 2008; 23:1698–1707.
9. Girouard J, Frenette G, Sullivan R. Comparative proteome and lipid profiles of bovine epididymosomes collected in the intraluminal compartment of the caput and cauda epididymis. Intl J Androl 2011; 34: e475–e486.
10. Wennemuth G, Babcock DF, Hille B. Expression and localization of pmca4 in rat testis and epididymis. J Gen Physiol 2003; 122:115–128.
11. Wilhelm B, Brandenburger T, Post H, Aumüller G. Expression and localization of *pmca4* in rat testis and epididymis. Histochem Cell Biol 2008; 129:331–343.
12. Brandenburger T, Strehler EE, Filoteo AG, Caride AJ, Aumüller G, Post G, Schwarz A, Wilhelm B. Switch of *pmca4* splice variants in bovine epididymis results in altered isoform expression during functional sperm maturation. J Biol Chem 2011; 286:7938–7946.
13. Di Leva F, Domi T, Fedrizzi L, Lim DH, Carafoli E. The plasma membrane Ca2+ ATPase of animal cells: structure, function and regulation. Arch Biochem Biophys 2008; 476:65–74.
14. Okunade GW, Miller ML, Pyne GJ, Sutliff RL, O'Conner KT, Neumann JC, Andringa A, Miller DA, Prasad V, Doetschman T, Paul RJ, Shull GE. Targeted ablation of plasma membrane Ca2+ ATPase (PMCA) 1 and 4 indicates a major housekeeping function for Pmca1 and a critical role in hyperactivated sperm motility and male fertility for *Pmca4*. J Biol Chem 2004; 279:33742–33750.
15. Schuh K, Cartwright EJ, Jankevics E, Bundschu K, Liebermann J, Williams JC, Armesilla AL, Emerson M, Oceandy D, Knobeloch KP, Neyses L. Plasma membrane Ca2+ ATPase 4 is required for sperm motility and male fertility. J Biol Chem 2004; 279:28220–28226.
16. Caride AJ, Filoteo AG, Penniston JT, Strehler EE. The plasma membrane Ca^{2+} pmp isoform 4a differs from isoform 4b in the mechanism of calmodulin binding and activation kinetics. Implications for Ca^{2+} signaling. J Biol Chem 2007; 282:25640–25648.
17. DeMarco SJ, Strehler EE. Plasma membrane Ca^{2+}-ATPase isoforms 2b and 4b interact promiscuously and selectively with members of the membrane-associated guanylate kinase family of PDZ (PSD95/Dlg/ZO-1) domain-containing proteins. J Biol Chem 2001; 276:21594–21600.
18. Filoteo AG, Elwess NL, Enyedi A, Caride A, Aung HH, Penniston JT. Plasma membrane Ca^{2+} pump in rat brain. Patterns of alternative splices seen by isoform-specific antibodies. J Biol Chem 1997; 272: 23741–23747.
19. Zhang H, Jones R, Martin-DeLeon PA. Expression and secretion of a GPI-linked form of hyaluronidase in the rat epididymis: role of testicular lumicrine factors. Matrix Biol 2004; 22:653–661.
20. Deng X, He Y, Martin-DeLeon PA. Mouse Spam1 (Ph-20): evidence for its expression in the epididymis and for a new category of spermatogenic expressed genes. J Androl 2000; 21:822–832.
21. Zhang H, Martin-DeLeon PA. Mouse Epididymal SPAM1 (Ph-20) is released in vivo and in vitro, and Spam1 is differentially regulated in testis and epididymis. Biol Reprod 2001; 65:1586–1593.
22. Griffiths GS, Reese KL, Galileo DS, and Martin-DeLeon PA. Investigating the role of murine epididymosomes and uterosomes in GPI-linked protein transfer to sperm using SPAM1 as a model. Mol Reprod Dev 2008; 75:1627–1636.
23. Griffiths GS, Galileo DS, Aravindan RG, Martin-DeLeon PA. Clusterin facilitates exchange of glycosyl-phosphosphatidylinositol-linked SPAM1 between reproductive luminal fluids and mouse and human sperm membranes. Biol Reprod 2009; 81:562–570.
24. Kher R, Bacallao R. Direct in situ reverse transcriptase-polymerase chain reaction. Am J Physiol 2001; 281:C726–C732.
25. Molecular Techniques and Methods in Situ Reverse Transcription-Polymerase Chain Reaction (In Situ RT-PCR). Institute of Molecular Development LLC; 2001. http://www.molecularinfo.com/MTM/E/E3/E3-2.html. Accessed October 3, 2011.
26. Aravindan RG, Fomin VP, Naik UP, Galileo DS, Naik MU, Modelski MJ, Duncan RL, Martin-DeLeon PA. CASK interacts with PMCA4b and JAM-A on the mouse sperm flagellum to regulate Ca^{2+} homeostasis and motility. J Cell Physiol 2012; 227:3138–3150.
27. Zhang H, Martin-DeLeon PA. Mouse epididymal Spam1 (PH-20) is released in the luminal fluid with its lipid anchor. J Androl 2003; 24: 51–58.
28. Maldera JA, Vasen G, Ernesto JL, Weigel-Munoz M, Chen DJ, Cuasincu PS. Evidence for the involvement of zinc in the association of CRISP1 with rat sperm during epididymal maturation. Biol Reprod 2011; 85: 503–510.
29. Keeton TP, Shull GE. Primary structure of rat plasma membrane Ca^{2+}-ATPase isoform 4 and analysis of alternative splicing patterns at splice site A. Biochem J 1995; 306:779–785.
30. Strehler EE, Zacharias DA. Role of alternative splicing in generating isoform diversity among plasma membrane calcium pumps. Physiol Rev 2001; 81:21–50.
31. Withers S, Cartwright EJ, Neyes L. Sperm phenotype of mice carrying a gene deletion for the plasma membrane calcium/calmodulin dependent ATPase 4. Mol Cell Endocrinol 2006; 250:93–97.
32. Enyedi AJ, Verma AK, Heim RA, Adamo HP, Filoteo AJ, Strehler EE, and Penniston JT. The Ca2+ affinity of the plasma membrane Ca2+ pump is controlled by alternative splicing. J Biol Chem 1994; 269:41–43.
33. Cooper TG. Epididymis and sperm function. Andrologia 1996; 28:57–59.
34. Belan PV, Gerasimenko OV, Tepikin AV, Petersen OH. Localization of Ca^{2+} extrusion sites in pancreatic acinar cells. J Biol Chem 1996; 271: 7615–7619.
35. Lee MG, Xu X, Zeng W, Diaz J, Kuo TH, Wuytack F, Racymaekers L, Muallem S. Polarized expression of Ca^{2+} pumps in pancreatic and salivary gland cells. Role in initiation and propagation of $[Ca^{2+}]i$ waves. J Biol Chem 1997; 272:15771–15776.
36. Post H, Wiche R, Sen PC, Hoffbauer G, Albrecht M, Seitz J, Aumuller G, Wilhelm B. Identification of a plasma membrane Ca^{2+}-ATPase in epithelial cells and aposomes of the rat coagulating gland. Prostate 2002; 52:159–166.
37. Reinhardt TA, Filoteo AG, Penniston JT, Horst RL. Ca(2+)-ATPase protein expression in mammary tissue. Am J Physiol Cell Physiol 2000; 279:C1595–C1602.
38. Setchell BP, Maddocks S, Brooks DE. Anatomy, vasculature, innervation and fluids of the male reproductive tract In: Knobil E, Neill JD (eds.), The Physiology of Reproduction, vol. 1, 2nd ed. New York: Raven Press; 1994;1063–1175.
39. Anakwe OO, Sharma S, Hoff HB, Hardy DM, Gerton GL. Maturation of guinea pig sperm in the epididymis involves the modification of proacrosin oligosaccharide side chains. Mol Reprod Dev 1991; 29: 294–301.
40. Bedford JM, Hoskins DD. The mammalian spermatozoon morphology, biochemistry and physiology In: Lamming GE (ed.), Marshall's Physiology of Reproduction, vol. 2, 4th ed. London: Churchill Livingstone; 1990;370–568.

41. Soler C, Yeung CH, Cooper TG. Development of sperm motility in the murine epididymis. Int J Androl 1994; 17:271–278.
42. Hermo L, Jacks D. Nature's ingenuity: bypassing the classical secretory route via apocrine secretion. Mol Reprod Dev 2002; 63:394–410.
43. Saez FJ, Frenette GP, Sullivan RM. Epididymosomes and prostasomes: their roles in post-testicular maturation of the sperm cells. J Androl 2003; 24:149–154.
44. Frenette GP, Sullivan RM. Prostasome-like particles are involved in the transfer of P25b from the bovine epididymal fluid to the sperm surface. Mol Reprod Dev 2001; 59:115–121.
45. Yeung CH, Cooper TG. Acquisition and development of sperm motility upon maturation in the epididymis. In: Robaire B, Hinton BT (eds.), The Epididymis: From Molecules to Clinical Practice. New York: Kluwer Academic/Plenum Publishers; 2002:417–434.
46. Rejraji H, Sion BA, Prensier G, Carreras MC, Motta CT, Frenoux JM, Vericel E, Grizzard G, Vernet P, Drevet JR. Lipid remodeling of murine epididymosomes and spermatozoa during epididymal maturation. Biol Reprod 2006; 74:1104–1113.
47. Strehler EE, Caride AJ, Filoteo AG, Xiong Y, Penniston JT, Enyedi A. Plasma membrane Ca2+ ATPases as dynamic regulators of cellular calcium handling. Ann N Y Acad Sci 2007; 1099:226–236.
48. Shao M, Ghosh A, Cooke VG, Naik UP, Martin-DeLeon PA. JAM-A is present in mammalian spermatozoa where it is essential for normal motility. Dev Biol 2008; 313:246–255.
49. Kosk-Kopsicka D, Bzdega T. Activation of the erythrocyte Ca2+-ATPase by either self-association or interaction with calmodulin. J Biol Chem 1988; 263:18184–18189.
50. Vorherr T, Kessler T, Hofmann F, Carafoli E. The calmodulin-binding domain mediates the self-association of the plasma membrane Ca2+ pump. J Biol Chem 1991; 266:22–27.
51. Levi V, Rossi JP, Castello PR, Gonzalez Flecha FL. Oligomerization of the plasma membrane calcium pump involves two regions with different thermal stability. FEBS Lett 2003; 483:99–103.
52. Funke L, Dakoji S, Bredt DS. Membrane-associated guanylate kinases regulate adhesion and plasticity at cell junctions. Annu Rev Biochem 2005; 74:219–245.
53. Kim EY, DeMarco SJ, Marfatia SM, Chishti AH, Sheng M, Strehler EE. Plasma membrane Ca2+ ATPase isoform 4b binds to membrane-associated guanylate kinase (MAGUK) proteins via their PDZ (PSD-95/Dlg/ZO-1). J Biol Chem 1998; 273:1591–1595.